# Short-Time Spin Dynamics in Strongly Correlated Few-Fermion Systems

Sebastiano Peotta, Davide Rossini, Pietro Silvi, G. Vignale, Rosario Fazio, and Marco Polini

# Short-time spin dynamics in strongly correlated few-fermion systems

Sebastiano Peotta,[1] Davide Rossini,[1] Pietro Silvi,[2] G. Vignale,[3] Rosario Fazio,[1] and Marco Polini[4]

[1]*NEST, Scuola Normale Superiore and Istituto di Nanoscienze-CNR, I-56126 Pisa, Italy*
[2]*International School for Advanced Studies (SISSA), Via Bonomea 265, 34136 Trieste, Italy*
[3]*Department of Physics and Astronomy, University of Missouri, Columbia, Missouri 65211, USA*
[4]*NEST, Istituto di Nanoscienze-CNR and Scuola Normale Superiore, I-56126 Pisa, Italy*

The non-equilibrium spin dynamics of a one-dimensional system of repulsively interacting fermions is studied by means of density-matrix renormalization-group simulations. We focus on the short-time decay of the oscillation amplitudes of the centers of mass of spin-up and spin-down fermions. Due to many-body effects, the decay is found to evolve from quadratic to linear in time, and eventually back to quadratic as the strength of the interaction increases. The characteristic rate of the decay increases linearly with the strength of repulsion in the weak-coupling regime, while it is inversely proportional to it in the strong-coupling regime. Our predictions can be tested in experiments on tunable ultra-cold few-fermion systems in one-dimensional traps.

*Introduction.* — In an electron liquid the motion of one of the two spin species, *e.g.* in the presence of a spin current, can drag along the other one because of electron-electron interactions. This is the spin Coulomb drag effect or simply the *Spin Drag* (SD) [1–3]. In electron transport SD can be described by a frictional force proportional to the difference between the velocities of the two populations and is described by a damping term in the equation of motion for the time derivative of the spin-resolved center-of-mass momentum. SD has been observed [4, 5] in two-dimensional electron gases in semiconductor heterojunctions.

The concept of SD can be extended to other quantum fluids with distinguishable species that can exchange momentum due to mutual collisions. Ultracold atomic gases [6] are clean systems in which SD can be observed in a truly *intrinsic* regime [7–11]. Further, the interaction strength between atoms can be tuned at will by employing Feshbach resonances [6].

This Letter is motivated by a recent pioneering experiment [12] on SD in an equal mixture of two hyperfine states of $^6$Li atoms confined in a trap. The authors of Ref. 12 measured independently the time-dependent position of the centers of mass of "spin-up" and "spin-down" particles starting from an initial condition in which the two types of particles are grouped in well-separated clouds. The experiment is performed in the "unitarity limit" in which the strength of interactions is the largest possible. At long times the separation of the centers of mass decays exponentially to zero. By measuring the time constant of this exponential decay the SD coefficient is determined.

Besides providing information on SD in the strong coupling regime, Ref. 12 provides a wealth of new data on the *short-time* behavior – long before the SD regime is attained. There it is found that the two clouds perform several cycles of oscillation before settling at the bottom of the trap. If interactions are sufficiently strong,

they reflect off each other several times before the interdiffusion process begins. This short-time regime of spin dynamics, the short-time SD (STSD), constitutes the focus of the present Letter. We tackle it non-perturbatively by the time-dependent density-matrix renormalization group (tDMRG) method [13, 14]. This method is essentially exact, its main limitation being the maximum system size that we can handle [15]. Starting from an initial condition similar to that of Ref. 12, we find that the oscillation amplitudes of the centers of the spin clouds decay in time *quadratically* for weak interactions, *linearly* for intermediate interactions, and again quadratically for very large interactions. Below we argue that this intriguing reentrant behavior is a many-body effect. Our predictions are amenable to experimental testing, since in a recent work Serwane *et al.* [16] were able to trap few fermions in a 1D geometry and to tune their mutual interactions by means of a Feshbach resonance.

*The model.* — We consider a two-component fermion system with repulsive short-range interactions in a 1D trap. The system is prepared in the ground state of two (spin-dependent) displaced harmonic potentials [Fig. 1a]. At time $t = 0^+$ these external potentials are *suddenly* turned off and the system evolves in presence of a single harmonic confinement, according to the Fermi-Hubbard (FH) Hamiltonian,

$$\hat{\mathcal{H}} = -J \sum_{i,\sigma} (\hat{c}_{i,\sigma}^\dagger \hat{c}_{i+1,\sigma} + \text{H.c.}) + U \sum_i \hat{n}_{i,\uparrow} \hat{n}_{i,\downarrow} + \sum_i W_i \hat{n}_i \, .$$

$$(1)$$

Here $J$ is the inter-site hopping parameter, $\hat{c}_{i,\sigma}^\dagger$ ($\hat{c}_{i,\sigma}$) creates (destroys) a fermion in the $i$-th site ($i \in [1, L]$, $L$ being the total number of lattice sites), $\sigma = \uparrow, \downarrow$ is a label for a pseudospin-1/2 (hyperfine-state) degree of freedom, $U > 0$ is the on-site repulsion, $\hat{n}_{i,\sigma} = \hat{c}_{i,\sigma}^\dagger \hat{c}_{i,\sigma}$ is the local spin-resolved number operator, and $\hat{n}_i = \hat{n}_{i,\uparrow} + \hat{n}_{i,\downarrow}$. The third term on the r.h.s. of Eq. (1) represents an external parabolic potential $W_i = V_2(i - L/2)^2$ of strength $V_2$,

corresponding to a frequency $\omega = 2\sqrt{V_2 J}/\hbar$.

We follow the time-evolution of the spin-resolved densities $\langle \hat{n}_{i,\sigma}(t) \rangle$ on a time scale much smaller than the spin equilibration time [17] and calculate the spin-resolved centers of mass from $X_{\mathrm{CM},\sigma}(t) \equiv L^{-1} \sum_{i=1}^{L} (i - L/2) \langle \Psi(t) | \hat{n}_{i,\sigma} | \Psi(t) \rangle$.

*Results and discussion.* — In Fig. 1 we illustrate the time evolution of the occupation numbers $n_{i,\sigma}(t)$ for a system of $N = 6$ spin-up particles and $N = 6$ spin-down particles, in a lattice with $L = 240$ sites. The harmonic potential has a strength $V_2/J = (1/160)^2$, corresponding to a harmonic oscillator length $\bar{a}_{\mathrm{ho}} = (J/V_2)^{1/4} \approx 12.65$, in units of the lattice constant, and to a frequency $\omega = J/(80\hbar)$. These parameters have been used also for all other plots and their choice yields minimal lattice effects (see below) [18]. The data in Fig. 1 correspond to $U/J = 5$. In panel a) we illustrate the initial state, with two non-overlapping clouds with opposite spins. Panels b)-f) show the time evolution of this initial state. We highlight two features: i) in panels b) and e) high-density regions form near the center of the trap due to strong repulsive interactions [12]; ii) in panels c), d), and f) we see how the spin-up cloud (blue curve) drags along a substantial fraction of down-spin atoms (red curve).

In Fig. 2a) we show the time evolution of spin-resolved center-of-mass, $X_{\mathrm{CM},\sigma}(t)$, *in the weak coupling regime*, $U/J \leq 0.05$. In absence of the lattice, the center-of-mass of each atomic cloud is decoupled from "internal" degrees of freedom and should oscillate at the trap frequency, $\omega$, without decaying. This is confirmed by the data corresponding to $U/J = 0$ in Fig. 2a) (dotted lines). No visible damping effects appear within the time-scale of the plot, since we have minimized lattice effects [19].

When $U/J$ is finite the two clouds still go through each other, but their motion is damped. Fig. 2b) reports the maxima of the blue and red curves as a function of time, for several different values of $U/J \leq 0.05$. The amplitude of the oscillations in Fig. 2a) decays quadratically in time. This is because, in this regime, the center of mass of each cloud is a harmonic oscillator weakly coupled to internal degrees of freedom. The relevant excitation spectrum, $\mathcal{S}(\Omega)$, is sharply peaked about $\Omega \sim \omega$. The position of the peak determines the frequency of the oscillations and the second moment of the spectrum determines the quadratic decay of their amplitude. The quadratic decay can be also verified analytically by means of time-dependent perturbation theory – see Sect. II in Ref. 14.

We now discuss the strongly correlated regime, $U/J \gg 1$. The main results are summarized in Fig. 3. Dotted lines in Fig. 3a) represent the exact time evolution of the spin-resolved center-of-mass for $U/J = \infty$. In this limit, the Hamiltonian in Eq. (1) maps onto [20] $\hat{\mathcal{H}}_\infty = -J\hat{\mathcal{P}} \sum_{i,\sigma} (\hat{c}_{i,\sigma}^\dagger \hat{c}_{i+1,\sigma} + \mathrm{H.c.})\hat{\mathcal{P}}$, where $\hat{\mathcal{P}}$ is a Gutzwiller projector (that avoids double occupation of a
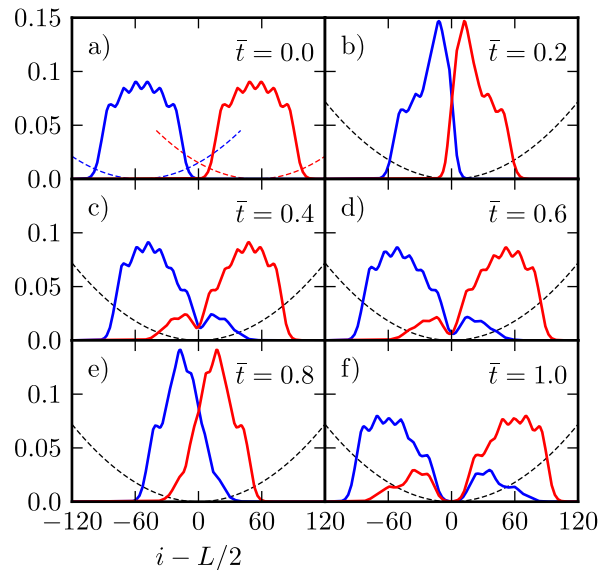


FIG. 1: (Color online) Time evolution of the site occupations $n_{i,\sigma}(t)$ for a system of twelve fermions at strong coupling ($U/J = 5$). Panel a) Initial state: two clouds of atoms with opposite spin (blue and red curves) are spatially separated using two displaced harmonic potentials. Panels b)-f) Subsequent time evolution after the abrupt switch-off of these local potentials. The two clouds are forced to propagate against each other in presence of an overall harmonic confinement of frequency $\omega$. The parameter $\bar{t}$ denotes time in units of the period $T = 2\pi/\omega$ induced by the harmonic confinement. Dashed lines indicate the initial spin-dependent displaced harmonic traps [panel a)] and the overall harmonic trap for $t > 0$ [panels b)-f)], and are plotted as guides to the eye.

lattice site). Dotted lines have been obtained by applying tDMRG to $\hat{\mathcal{H}}_\infty$. Notice that the centers of mass of the two clouds behave practically like two classical particles that bounce off each other quasi-elastically oscillating at twice the trap frequency. The frequency doubling with respect to Fig. 2a) is understandable as follows. Due to strong repulsion, fermions of opposite spin are confined to one half of the trap: effectively, only the antisymmetric levels of the harmonic oscillator, whose energy separation is $2\omega$, are involved in the time evolution. A rather complicated dynamical pattern, however, is present in the time evolution of the spin-resolved site occupations $n_{i,\sigma}(t)$ (see Fig. 1).

In Fig. 3b) we plot the amplitude of oscillations vs time for $5 \leq U/J \leq 30$. Remarkably they decay *linearly*. As mentioned in the Introduction, the quadratic-to-linear crossover is a many-particle effect. One can indeed solve analytically the evolution dynamics for an interacting system of *two* particles with antiparallel spin in a harmonic potential. In that case, the time evolution of $X_{\mathrm{CM},\sigma}$ follows the quadratic behavior seen in Fig. 2b), even for strong interactions (see Sect. III of
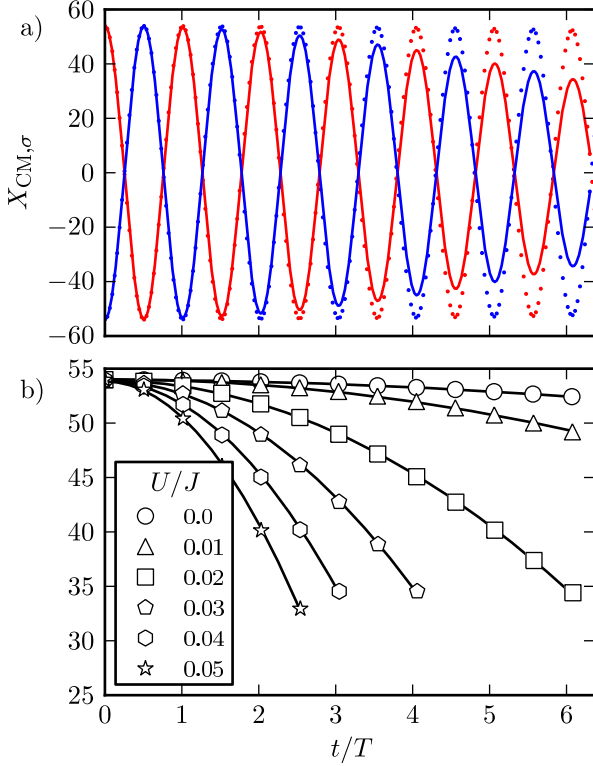
FIG. 2: (Color online) Panel a) Time evolution of the spin-resolved center-of-mass $X_{\mathrm{CM},\sigma}(t)$ of a system of twelve fermions in a harmonic potential. Solid lines refer to $U/J = 0.02$ while dotted lines to $U/J = 0$. Panel b) Positions of the maxima of the amplitude of the center-of-mass oscillations as functions of time $t$ in units of $T = 2\pi/\omega$. Different symbols correspond to different interaction strengths. The tiny decay in the non-interacting case is due to lattice effects. Solid lines are parabolic fits, $X_{\mathrm{CM},\sigma}(t)|_{\mathrm{peak}} = X_0 \left[1 - (t/\tau_{\mathrm{stsd}})^2\right]$, where $X_0$ is the same for all values of $U/J$.

FIG. 3: (Color online) Panel a) Same as in Fig. 2a) but at strong coupling. Solid (dashed) lines refer to $U/J = 20$ ($U/J = 5$) while dotted lines to $U/J = \infty$. In the latter case the oscillations have twice shorter periodicity than those of non-interacting fermions. Note that they do not display an appreciable decay on the time scale of the plot. Panel b) Same as in Fig. 2b) but at strong coupling. Solid lines are fits obtained by using Eq. (12) in Sect. IV of Ref. 14.

Ref. 14). With many particles, as the strength of the interaction increases, the centers of mass of the clouds become increasingly coupled to internal degrees of freedom. If $N$ is sufficiently large, $\mathcal{S}(\Omega)$ becomes featureless, with a bandwidth of the order of $\omega$. In this regime one has the situation of a single degree of freedom (center of mass) irreversibly transferring energy into a "bath" of microscopic degrees of freedom: accordingly, the amplitude of the oscillations decays linearly in time as expected of an ordinary damped oscillator.

These observations imply a non-trivial crossover in the short-time dynamics of $X_{\mathrm{CM},\sigma}(t)|_{\mathrm{peak}}$ as a function of the number of particles. In particular, as illustrated in Figs. 5-8 of Ref. 14 (Sect. IV), we note the existence of a time scale $t^\star$, depending on $N$ and $U/J$, below which the decay of the oscillation amplitudes is *quadratic*. The value of $t^\star$ decreases with increasing $N$ and increases with increasing $U/J$. More quantitatively, we have investigated such crossover by fitting numerical data at
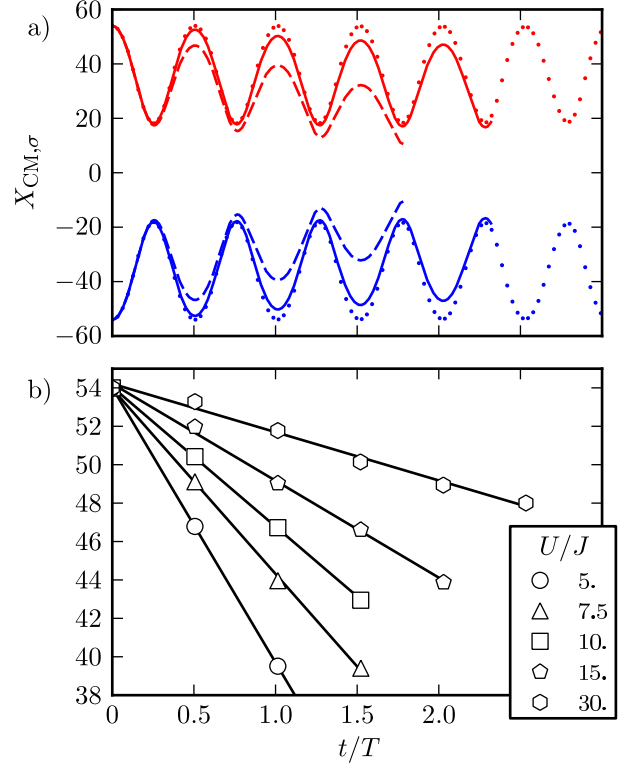
strong coupling with the "split-fit" formula in Eq. (12) of Ref. 14, which contains $\tau_{\mathrm{stsd}}$ and $t^\star$ as fitting parameters. This equation encodes a quadratic decay for $t \leq t^\star$, followed by a linear behavior for $t > t^\star$. From our analysis we conclude that the value of $t^\star$ for $N = 6$ and $5 \lesssim U/J \lesssim 30$ is much smaller than the period of oscillations. This explains why no quadratic behavior is seen in Fig. 3b). From the numerical data at strong coupling, we conclude that a linear decay in time of $X_{\mathrm{CM},\sigma}(t)|_{\mathrm{peak}}$ occurs when the overlap between the two colliding clouds is substantial, while a quadratic decay takes place initially (for $t < t^\star$) when minor overlap occurs in the tails of the clouds.

Our main results for the time scale $\tau_{\mathrm{stsd}}$ associated with STSD are summarized in Fig. 4. Here we report the values of $\tau_{\mathrm{stsd}}^{-1}$ used to produce the fits in Figs. 2b)-3b). We clearly see that $\tau_{\mathrm{stsd}}^{-1}$ vanishes linearly in the weak-coupling $U/J \rightarrow 0$ limit. This has to be contrasted with the SD relaxation rate in a system with many degrees of freedom at equilibrium: the latter is quadratic in the coupling constant governing the strength of inter-particle
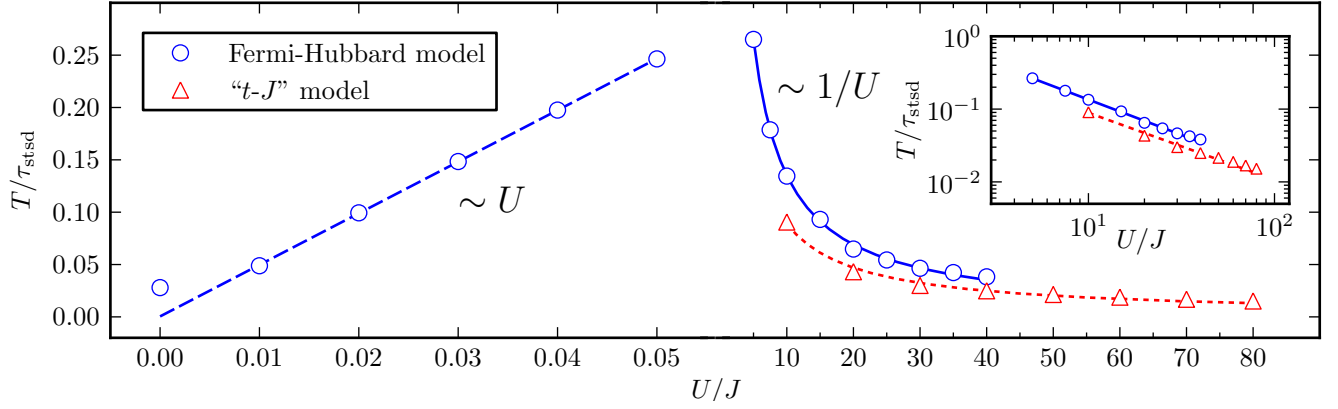
FIG. 4: (Color online) Empty circles represent the inverse of the short-time spin-drag time constant, $\tau_{\mathrm{stsd}}^{-1}$ (in units of $1/T$), as a function of the coupling $U/J$. These data have been extracted from the spin dynamics of the model (1) (quadratic fit at weak coupling and "split-fit" procedure at strong coupling, see Ref. 14). In a wide range of coupling constants, $0.1 \lesssim U/J \lesssim 1$, fittings like the ones in Figs. 2b)-3b) do not work. We see that $\tau_{\mathrm{stsd}}^{-1}$ vanishes linearly in the weak-coupling regime (long-dashed line) and behaves approximately like $1/U$ at strong coupling (solid line). The solid line is a power-law fit, $i.e.$ $1/\tau_{\mathrm{stsd}} = A\ (U/J)^{-\alpha}$, with $A \approx 1.26/T$ and $\alpha \approx 0.97$. The empty triangles label $\tau_{\mathrm{stsd}}^{-1}$ as extracted from the spin dynamics of the effective model (2). The short-dashed line is a power-law fit of the form $1/\tau_{\mathrm{stsd}} = B\ (U/J)^{-\beta}$, with $B \approx 0.7/T$ and $\beta \approx 0.91$. While the two exponents $\alpha$ and $\beta$ are very similar, the proportionality constants $A$ and $B$ are slightly different. This discrepancy may be due to the neglect of three-site terms [22] in Eq. (2). In the inset we show the same strong-coupling results in a log-log scale.

interactions (see $e.g.$ Ref. 7). In the strong-coupling limit $\tau_{\mathrm{stsd}}^{-1}$ behaves approximately like $1/U$. No analytical results are available in this regime, even in a system with many degrees of freedom at equilibrium. We emphasize that, for all the data at $U/J \gg 1$ in Fig. 4, $t^\star$ is within the observation time of our simulations.

To check the robustness of our conclusions at strong coupling, we study an effective "$t$-$J$" model [20, 21] which approximates (1) for $U/J \gg 1$:

$$\hat{\mathcal{H}}' = \hat{\mathcal{H}}_\infty + \frac{4J^2}{U} \sum_i \left( \hat{\boldsymbol{S}}_i \cdot \hat{\boldsymbol{S}}_{i+1} - \frac{\hat{n}_i \hat{n}_{i+1}}{4} \right) + \sum_i W_i \hat{n}_i \ , \tag{2}$$

where $\hat{\boldsymbol{S}}_i = \sum_\alpha \hat{c}_{i,\alpha}^\dagger (\boldsymbol{\sigma}_{\alpha\beta}/2)\hat{c}_{i,\beta}$ is the spin operator ($\boldsymbol{\sigma}$ being a three-dimensional vector of Pauli matrices) [22]. When $U/J \gg 1$ such model is much easier to simulate than the original FH model. Employing Eq. (2) we have discovered that, for a fixed value of $N$, the amplitude of the oscillations decays quadratically in time when $U/J$ is sufficiently large. This is shown in Fig. 5 of Ref. 14. In other words, as mentioned in the Introduction, the quadratic dependence on time of the decay of the oscillation amplitudes displays a reentrant behavior pertaining to the many-particle problem. In Fig. 4 we report the results for the inverse STSD time constant of the model (2) (empty triangles), which agree qualitatively with those based on the full FH model.

In summary, we studied short-time spin-density oscillations in a strongly-interacting 1D few-fermion system. We discovered that the decay in the oscillation amplitudes goes from quadratic to linear back to quadratic in time as the interaction strength increases from zero to

infinity. The inverses of the properly-defined time constants depend on the strength of inter-particle interactions in a way that was unpredictable on the basis of our knowledge of the same phenomenon in many-particle systems near equilibrium. Our predictions can be tested by studying the damping of spin-dipole oscillations in few-fermion systems [16].

[1] I. D'Amico and G. Vignale, Phys. Rev. B **62**, 4853 (2000); $ibid.$ **65**, 085109 (2002); $ibid.$ **68**, 045307 (2003).
[2] K. Flensberg, T.S. Jensen, and N.A. Mortensen, Phys. Rev. B **64**, 245308 (2001).
[3] For a short review see M. Polini and G. Vignale, Physics **2**, 87 (2009).
[4] C.P. Weber $et\ al.$, Nature **437**, 1330 (2005).
[5] L. Yang $et\ al.$, Nature Phys. **8**, 153 (2012).
[6] I. Bloch, J. Dalibard, and W. Zwerger, Rev. Mod. Phys. **80**, 885 (2008).
[7] M. Polini and G. Vignale, Phys. Rev. Lett. **98**, 266403 (2007); D. Rainis $et\ al.$, Phys. Rev. B **77**, 035113 (2008).
[8] Gao Xianlong $et\ al.$, Phys. Rev. Lett. **101**, 206402 (2008).
[9] G.M. Bruun $et\ al.$, Phys. Rev. Lett. **100**, 240406 (2008).
[10] R.A. Duine $et\ al.$, Phys. Rev. Lett. **104**, 220403 (2010).
[11] R.A. Duine and H.T.C. Stoof, Phys. Rev. Lett. **103**, 170401 (2009); H.J. van Driel, R.A. Duine, and H.T.C. Stoof, $ibid.$ **105**, 155301 (2010).
[12] A. Sommer $et\ al.$, Nature **472**, 201 (2011).
[13] See $e.g.$ U. Schollwöck, Ann. Phys. (NY) **326**, 96 (2011).
[14] Supplemental material file.

[15] The tDMRG method has been employed by several authors to study the dynamics of interacting fermions on a lattice: see *e.g.* F. Heidrich-Meisner *et al.*, Phys. Rev. A **78**, 013620 (2008); Wei Li *et al.*, Phys. Rev. B **78**, 195109 (2008); F. Heidrich-Meisner *et al.*, Phys. Rev. A **80**, 041603 (2009) and references therein. Similar dynamical studies to the ones performed in this work have been recently carried out by J. Kajala, F. Massel, and P. Törmä, Eur. Phys. J. D **65**, 91 (2011). The authors of this work set to zero the third term in Eq. (1) and do not focus on STSD (while they study the dynamics of pair formation for $U < 0$). The transmission probability in a setup like ours after a time $t = T/2$ has been studied by J. Ozaki, M. Tezuka, and N. Kawakami, arXiv:1107.0774. The expansion dynamics has been studied by J. Kajala, F. Massel, and P. Törmä, Phys. Rev. Lett. **106**, 206401 (2011) and by S. Langer *et al.*, arXiv:1109.4364. 3D hydrodynamic [E. Taylor *et al.*, Phys. Rev. A **84**, 063622 (2011)] and Boltzmann [O. Goulko, F. Chevy, and C. Lobo, Phys. Rev. A **84**, 051605 (2011)] approaches have been used to interpret the data in Ref. 12.

[16] F. Serwane *et al.*, Science **332**, 336 (2011).

[17] Here $\langle \hat{n}_{i,\sigma}(t) \rangle$ is a shorthand for $\langle \Psi(t) | \hat{n}_{i,\sigma} | \Psi(t) \rangle$, where $|\Psi(t)\rangle$ is the state of the system at time $t$.

[18] To achieve the continuum limit we need to consider a rather large number of sites and a sufficiently shallow harmonic confinement. This forces the quantum dynamics to be slow on the time scale of $\hbar/J$. As a matter of fact, with the parameters used throughout this Letter, the period induced by the harmonic confinement is $T = 160\pi(\hbar/J)$. Despite the intrinsic difficulty of tDMRG in addressing the long-time $t \gg \hbar/J$ limit, we are able to follow the dynamics up to $t \sim 6\,T$ thanks to the small number of particles ($2N \ll L$).

[19] A.M. Rey *et al.*, Phys. Rev. A **72**, 033616 (2005).

[20] T. Giamarchi, *Quantum Physics in One Dimension* (Clarendon Press, Oxford, 2004).

[21] F.H.L. Essler *et al.*, *The One-dimensional Hubbard Model* (Cambridge University Press, Cambridge, 2005).

[22] The mapping $\hat{\mathcal{H}} \to \hat{\mathcal{H}}'$ for $U/J \gg 1$ is, however, not exact since in writing Eq. (2) we have neglected three-site terms, which are difficult to simulate and potentially important away from half filling [21].